HHS Public Access

Author manuscript

J Cell Physiol. Author manuscript; available in PMC 2020 April 01.

Published in final edited form as:

J Cell Physiol. 2019 April ; 234(4): 4432–4444. doi:10.1002/jcp.27232.

Mitochondrial Dysfunction in HIV-1 Transgenic Mouse Cardiac Myocytes

Joseph Y. Cheung[1,2], **Jennifer Gordon**[3,4], **JuFang Wang**[1], **Jianliang Song**[1], **Xue-Qian Zhang**[1], **Fabian Jana Prado**[1], **Santhanam Shanmughapriya**[1,5], **Sudarsan Rajan**[1,5], **Dhanendra Tomar**[1,5], **Farzaneh G. Tahrir**[3,4], **Manish K. Gupta**[3,4], **Tijana Knezevic**[3,4], **Nana Merabova**[3,4], **Christopher D. Kontos**[6], **Joseph M. McClung**[7], **Paul E. Klotman**[8], **Muniswamy Madesh**[1,5], **Kamel Khalili**[3,4], and **Arthur M. Feldman**[2]

[1]Center of Translational Medicine, Lewis Katz School of Medicine of Temple University, Philadelphia, PA 19140

[2]Department of Medicine, Lewis Katz School of Medicine of Temple University, Philadelphia, PA 19140

[3]Department of Neuroscience, Lewis Katz School of Medicine of Temple University, Philadelphia, PA 19140

[4]Center for Neurovirology, Lewis Katz School of Medicine of Temple University, Philadelphia, PA 19140

[5]Department of Medical Genetics and Molecular Biochemistry, Lewis Katz School of Medicine of Temple University, Philadelphia, PA 19140

[6]Department of Medicine, Duke University School of Medicine, Durham, NC 27710

[7]Department of Physiology, Brody School of Medicine of East Carolina University, Greenville, NC27858

[8]Baylor College of Medicine, Houston, TX 77030

Abstract

The pathophysiology of human immunodeficiency virus (HIV)-associated cardiomyopathy remains uncertain. We used HIV-1 transgenic (Tg26) mice to explore mechanisms by which HIV-related proteins impacted on myocyte function. Compared to adult ventricular myocytes isolated from non-transgenic (WT) littermates, Tg26 myocytes had similar mitochondrial membrane potential (Δ_m) under normoxic conditions but lower $\Delta\Psi_m$ after hypoxia/reoxygenation (H/R). In addition, $\Delta\ \Psi_m$ in Tg26 myocytes failed to recover after Ca^{2+} challenge. Functionally, mitochondrial Ca^{2+} uptake was severely impaired in Tg26 myocytes. Basal and maximal oxygen

Address correspondence to: Joseph Y. Cheung, M.D., Ph.D., 3500 N. Broad Street, MERB 958, Philadelphia, PA 19140, Joseph.cheung@tuhs.temple.edu, Tel. 215-707-1799, Fax. 215-707-9890.

6. Conflict of Interest

KK is a board member, scientific advisor, and holds equity in Excision Biotherapeutics, a biotech start-up who has licensed the viral gene editing technology from Temple University for commercial development, and clinical trials. AMF and KK have a pending US patent #611934,483 for BAG3 as a target for heart failure therapy. AMF and JYC have a pending US patent #621205,990 for BAG3 composition and methods. Exclusive rights to the patents have been optioned by Temple University to Renovacor, Inc. AMF and JYC hold equity in Renovacor, Inc.

consumption rates (OCR) were lower in normoxic Tg26 myocytes, and further reduced after H/R. Complex I subunit and ATP levels were lower in Tg26 hearts. Post-H/R, mitochondrial superoxide ($O_2^{\cdot -}$) levels were higher in Tg26 compared to WT myocytes. Overexpression of Bcl2-associated athanogene 3 (BAG3) reduced $O_2^{\cdot -}$ levels in hypoxic WT and Tg26 myocytes back to normal. Under normoxic conditions, single myocyte contraction dynamics were similar between WT and Tg26 myocytes. Post-H/R and in the presence of isoproterenol, myocyte contraction amplitudes were lower in Tg26 myocytes. BAG3 overexpression restored Tg26 myocyte contraction amplitudes to those measured in WT myocytes post-H/R. Co-immunoprecipitation experiments demonstrated physical association of BAG3 and the HIV protein *Tat*. We conclude: (i) under basal conditions, mitochondrial Ca^{2+} uptake, OCR and ATP levels were lower in Tg26 myocytes; (ii) post-H/R, $\Delta\Psi_m$ was lower, mitochondrial $O_2^{\cdot -}$ levels were higher, and contraction amplitudes were reduced in Tg26 myocytes; (iii) BAG3 overexpression decreased $O_2^{\cdot -}$ levels and restored contraction amplitudes to normal in Tg26 myocytes post-H/R in the presence of isoproterenol.

Keywords

mitochondria bioenergetics; HIV cardiomyopathy; adenovirus; adult myocyte culture; reactive oxygen species

1. Introduction

The introduction of highly active anti-retroviral therapy (HAART) in the 1990's, now referred to as combination anti-retroviral therapy (cART), has changed human immunodeficiency virus type 1 (HIV-1) infection from an acute and highly lethal malady into a chronic disease with much improved life expectancy (Mocroft et al. 2003). The improved virologic control achieved with cART, together with prompt and effective treatment of opportunistic infections, highlight the urgent need to understand the pathogenesis and devise effective treatment for complications of chronic HIV-1 infection such as HIV-1 associated cardiomyopathy. The phenotype of HIV-1 associated cardiomyopathy has shifted from primarily symptomatic dilated cardiomyopathy in the pre-HAART era to minimally symptomatic, mildly reduced left ventricular (LV) systolic function or diastolic dysfunction in the post-HAART era in developed countries (Remick et al. 2014). However, in developing countries where cART is not readily available and in a significant percentage of aged patients in the United States, HIV-1 infection still carries a significantly increased risk of developing heart failure with reduced ejection fraction even after adjustment for various confounders (Freiberg et al. 2017). Direct HIV-1 infection of cardiac myocytes (Grody et al. 1990, Lipshultz et al. 1990), vascular endothelial cells (Manga et al. 2017) and vascular smooth muscle cells (Eugenin et al. 2008), autoimmune mechanisms (Currie and Boon 2003), pro-inflammatory cytokines et al. 1999, Pozzan et al. 2009), uptake of HIV proteins released by adjacent infected cells (Fiala et al. 2004), and cardiotoxicity of antiviral medications (Comereski et al. 1993, McKenzie et al. 1995, Brinkman et al. 1998), have all been postulated to contribute to the development of HIV-1 associated cardiomyopathy. The cellular and molecular mechanisms by which chronic HIV-1 infection causes cardiac dysfunction remain unknown.

The hemizygous NL4–3Δ*gag/pol* transgenic (Tg26) mouse contains an internal deletion of the *gag/pol* coding sequence that renders the viral construct replication-deficient, non-infectious, and is an useful model to study the chronic effects of HIV-1 persistence (Klotman and Notkins 1996). Tg26 mice manifest HIV-1 associated nephropathy (Kopp et al. 1992), wasting, and skin lesions that phenotypically resemble their clinical counterparts in HIV-1 infected patients (Lewis 2003). Tissue extracts from Tg26 mice demonstrate the presence of HIV proteins such as *Tat, rev, nef, vif, vpr,* and *vpu* (Kopp et al. 1992, Niu et al. 2014). Focusing on cardiac function, under basal conditions, contractility of Tg26 mice of both FVB/N (aged 12 to 16 weeks)(Lewis et al. 2000) and C57BL/6J (aged 16 to 18 weeks) (Cheung et al. 2015) backgrounds are similar to that observed in non-transgenic littermates (WT). When challenged with stress such as open heart surgery, both maximal first time derivative of LV pressure rise (+dP/dt) and fall (-dP/dt) in Tg26 hearts do not recover to pre-operative levels, in contrast to that observed in WT hearts (Cheung et al. 2015). Similarly, after treatment with zidovudine for 21 days, biomarkers of early heart failure such as increases in atrial natriuretic factor mRNA and decreases in sarcoplasmic reticulum Ca^{2+}-ATPase mRNA are observed in male Tg26 but not in male WT hearts (Lewis et al. 2000). More pertinent to our present study is the observation that compared to WT hearts, Tg26 hearts exhibit a fourfold increase in the percent of mitochondria with ultra-structural damage (cristae dissolution and disruption) under basal conditions. After 35 days of zidovudine treatment, the number of damaged mitochondria is much higher in Tg26 compared to WT hearts (Lewis et al. 2000). The absence of infectious virus (simulating virologic control with cART), the normal cardiac function at baseline (simulating the minimally symptomatic and mildly reduced LV function in many HIV-1 infected patients in the post-HAART era), the presence of ultra-structural damage and biomarkers of early heart failure, and induction of overt cardiac dysfunction with either stress or anti-viral agents, continue to make the Tg26 mouse a relevant clinical model for the study of HIV-1 associated cardiomyopathy in the 21st century.

The Bcl2-associated athanogene 3 (BAG3) is a 575 amino acid anti-apoptotic protein that is constitutively expressed in the brain, heart, skeletal muscle and some cancers (Rosati et al. 2011). Its pleotropic effects are due to the presence of multiple protein binding motifs. Studies in cancer cells have shown that BAG3 is critical for protein quality control by serving as a co-chaperone with the large and small heat shock proteins, is anti-apoptotic through binding to Bcl2, and regulates cell migration, adhesion, metastasis, and proliferation (Behl 2016). In cardiac myocytes, BAG3 is intimately involved in the regulation of autophagy and apoptosis (Su et al. 2016), mitochondrial quality control (Tahrir et al. 2017), excitation-contraction coupling (Feldman et al. 2016), and sarcomere stability (Ulbricht and Hohfeld 2013). BAG3 levels are reduced in pigs, mice and humans with heart failure (Knezevic et al. 2015). Overexpression of BAG3 improves cardiac contractile dysfunction in mice post-ischemia/reperfusion (Su et al. 2016) and post-infarction (Knezevic et al. 2016). The potential interplay between BAG3 and HIV-1 was suggested by our observations that BAG3 overexpression rescues contractile abnormalities in adult mouse myocytes expressing the HIV-1 protein *Tat* and that BAG3 down-regulation by shRNA in Tg26 hearts severely reduces contractility (Cheung et al. 2015). In addition, the HIV-1 protein *Tat* impairs mitochondrial Ca^{2+} uptake, reduces oxygen consumption rate (OCR) and increases reactive

oxygen species (ROS) in neonatal rat ventricular myocytes (NRVMs)(Tahrir et al. 2018). The current study was undertaken to evaluate whether mitochondrial dysfunction is present in adult Tg26 cardiac myocytes, and whether BAG3 overexpression can rescue contractile dysfunction by improving mitochondrial redox state.

2. Materials and Methods

2.1 Tg26 mice and animal care

Hemizygous Tg26 mice (FVB/N backcrossed to C57BL/6J for at least six generations) (Cheung et al. 2015) at 16–18 weeks of age were used throughout this study. Non-transgenic littermates were used as wild-type (WT) controls. Mice were housed and fed on a 12 h:12 h light-dark cycle at Temple University Animal Facility and were supervised by veterinary staff members. Standard care was provided to all mice used for experiments. All protocols applied to the mice in this study were approved and supervised by the Institutional Animal Care and Use Committee at Temple University.

It should be pointed out that Tg26 mice in the original studies by Klotman (Klotman and Notkins 1996, Lewis et al. 2000) were on the FVB/N background and they developed a broad range of HIV-associated pathologies including HIV-associated nephropathy (HIVAN), wasting, cutaneous lesions, as well as myopathy/myositis (Lewis 2003). In addition, Tg26 mice on the FBV/N background showed early lethality at approximately 6–9 months of age. By contrast, Tg26 mice backcrossed to the C57Bl/6J background demonstrated normal lifespan (survival of at least 12 months) and renal function (normal blood urea nitrogen and creatinine, unpublished observations). There were occasional cutaneous lesions in Tg26 mice on the C57Bl/6J background but the overall phenotype was considerably milder than that on the FVB/N background. In this context, it is interesting to note that post-myocardial infarction (MI), survival of C57Bl/6J strain was higher compared to FVB/N strain (van den Borne et al. 2009). In particular, early lethal heart failure (between days 2 and 7 post-MI) occurred mainly in the FVB/N mice (28%) compared to C56Bl/6J mice (<10%). It has also been established that different mouse genetic backgrounds influenced ex vivo and in vivo cardiac function (Barnabei et al. 2010), as well as intracellular calcium regulation in the heart (Shah et al. 2010).

2.2 Isolation, adenoviral infection, and culture of adult murine cardiac ventricular myocytes

Cardiac myocytes were isolated from the septum and left ventricular (LV) free wall of Tg26 or WT mice according to the protocol of Zhou et al. (2000). Myocytes were either placed in suspension or plated on laminin-coated glass coverslips (Tucker et al. 2006, Song et al. 2008). Myocytes were used on the same day (within 2 to 6 hours after isolation) or after 24 hours of culture.

To express exogenous genes via adenovirus (Adv)-mediated gene transfer, two hours after isolation, myocytes were infected with replication-deficient Adv expressing either green fluorescent protein (GFP)(Adv-GFP, 6.6×10^6 pfu/ml) or BAG3 (Adv-BAG3, 2.0×10^6 pfu/ml) in 1 ml of fetal bovine serum-free Eagle minimal essential medium (MEM)

containing 0.2% bovine serum albumin (BSA), creatine (5 mM), carnitine (2 mM), taurine (5 mM), NaHCO3 (4.2 mM), penicillin (30 mg/L), gentamicin (4 mg/L), insulin-transferrin-selenium supplement, and 2,3-butanedione monoxime (BDM, 10 mM) for 3 hours. An additional ml of MEM (with same supplements) was then added, and myocytes were cultured for 24h before experiments (Song et al. 2008, Cheung et al. 2015). Before measurements of mitochondrial function and myocyte contraction, cells were bathed with MEM without BDM and returned to the incubator (37°C) for 30 min. We have previously demonstrated that under our culture conditions, adult mouse LV myocytes cultured for up to 48h maintained rod-shape morphology, transverse-tubule organization, and normal contractile function; and that infection with Adv-GFP had no effect on single myocyte contractility compared to uninfected myocytes (Song et al. 2008).

2.3 Hypoxia/Reoxygenation (H/R) protocol

To simulate ischemia/reperfusion in vitro, freshly isolated LV myocytes from WT and Tg26 hearts were exposed to either 21% O_2:5% CO_2 (normoxia) or 1% O_2:5% CO_2 (hypoxia) for 2h followed by 30 min. of reoxygenation (Miller et al. 2013, Miller et al. 2014). Myocytes were incubated in Krebs-Henseleit bicarbonate buffer containing 5 mM of pyruvate as the sole substrate (Cheung et al. 1982). For cultured adult myocytes, we have previously determined the optimal hypoxic exposure to be 30 min. followed by 30 min. of reoxygenation (Hoffman et al. 2015).

2.4 Measurement of mitochondrial membrane potential ($\Delta\Psi_m$) and mitochondrial Ca^{2+} uptake in permeabilized myocytes

Freshly isolated LV myocytes from WT and Tg26 mice were subjected to 2h of either normoxia or H/R. After gentle centrifugation, myocytes were transferred to an intracellular-like medium containing (in mM): 120 KCl, 10 NaCl, 1 KH_2PO_4, 20 4-(2-hydroxyethyl)-1-piperazine-ethanesulfonic acid (HEPES)-Tris, 10 succinate, thapsigargin (2 ¼g/ml), digitonin (80 ¼g/ml), pH 7.2, and protease inhibitors (EDTA-free complete tablets, Roche Applied Science). Fura-FF (0.5 ¼M) was added at 0 s, and JC-1 (800 nM)(both from Molecular Probes) was added at 20s to measure extra-mitochondrial Ca^{2+} and $\Delta\Psi_m$, respectively. Fluorescence signals were monitored in a temperature-controlled (37°C) multi-wavelength excitation (ex) and dual wavelength emission (em) spectrofluorometer (Delta RAM, Photon Technology Int.) using 490-nm ex/535-nm em for the monomer, 570-nm ex/595-nm em for the J-aggregate of JC-1, and 340- and 380-nm ex/510-nm em for Fura-FF. The ratiometric dye Fura-FF was calibrated as previously described (Mallilankaraman et al. 2012, Miller et al. 2014). At 450 s, 10 ¼M Ca^{2+} pulse was added, and $\Delta\Psi_m$ and extra-mitochondrial Ca^{2+} were monitored simultaneously. $\Delta\Psi_m$ was calculated as the ratio of the fluorescence of the JC-1 oligomeric to monomeric forms. Cytosolic Ca^{2+} clearance rate was taken to represent mitochondrial Ca^{2+} uptake.

2.5 Measurement of mitochondrial oxygen consumption rate (OCR) and ATP levels

Oxygen consumption rate in freshly isolated adult LV myocytes was measured at 37°C in an XF96 extracellular flux analyzer (Seahorse Bioscience)(Miller et al. 2014). Myocyte suspensions were sequentially exposed to oligomycin, carbonyl cyanide 4-(trifluoromethoxy)phenylhydrazone (FCCP), and rotenone plus antimycin A using the XF

Cell Mito Stress Kit (Seahorse Bioscience) according to the manufacturer's instructions. We have previously determined the optimal myocyte seeding density to be 10^4 cells/well (well diameter 8.1 mm top/3.81 mm bottom, well depth 15.49 mm, maximal volume 250 ¼l) (Miller et al. 2014).

ATP levels (luminescence) were measured in heart homogenates from either WT or Tg26 mice using a CellTiter-Glo luminescent cell viability assay kit as described previously (Irrinki et al. 2011, Miller et al. 2014).

2.6 Confocal mitochondrial ROS and $\Delta\Psi_m$ measurement in intact myocytes

Freshly isolated LV myocytes were loaded with the mitochondrial $\Delta\Psi_m$ indicator tetramethylrhodamine methyl ester (TMRM, 15 nM; Invitrogen). For cultured myocytes expressing either GFP or BAG3, after 30 min. of normoxia or hypoxia, during the reoxygenation phase cells were loaded with the mitochondrial superoxide-sensitive fluorophore MitoSOX Red (22 ¼M; Invitrogen) in the extracellular media containing 2% BSA, 0.06% pluronic acid, and 20 ¼M sulfinpyrazone at 37°C for 30 min. Cells were then washed, resuspended in the extracellular medium containing 0.25% BSA, and imaged using a Carl Zeiss Meta 510 confocal microscope with a 40X oil objective with 1.7X digital zoom at 548-nm ex/574-nm em and 510-nm ex/580-nm em for TMRM and MitoSOX Red, respectively (Mukhopadhyay et al. 2007, Miller et al. 2014).

2.7 Myocyte shortening measurements

LV myocytes (freshly isolated or cultured) adherent to laminin-coated glass coverslips were bathed in 0.6 ml of air- and temperature equilibrated (37°C), HEPES-buffered (20 mM, pH 7.4) medium 199 containing 1.8 mM $[Ca^{2+}]_o$. Myocytes were electrically paced to contract at 2 Hz and myocyte motion was captured by charge-coupled device video camera (Ionoptix; Milton, MA). Isoproterenol (Iso), when indicated, was present at 1 ¼M. Myocyte contraction dynamics was analyzed off-line with edge-detection algorithm as previously described (Tucker et al. 2006, Song et al. 2008, Cheung et al. 2015).

2.8 Immunoblotting

Mouse LV homogenates (Tucker et al. 2006) and myocyte lysates (Song et al. 2008) were prepared as previously described. Proteins were separated in 10% polyacrylamide gel under reducing (5% mercaptoethanol) conditions. Primary antibodies were rabbit polyclonal BAG3 antibody (1:1,000; Proteintech Group Inc, Chicago, IL) and anti-NDUFA4L2 (1:1,000; Abcam, Cambridge, MA). Calsequestrin was used as a loading control. Blots were washed and incubated with secondary antibody conjugated to horse radish peroxidase. Enhanced chemiluminescence (Amersham) was used for the detection of signals.

2.9 Co-immunoprecipitation

H9C2 cardiomyocytes were transfected with pcDNA6 myc-BAG3 or pcDNA3 *Tat*, or both plasmids for 48 hours. Cardiomyocytes were harvested in lysis buffer containing (in mM): 50 Tris pH 7.4, 150 NaCl, 1 EDTA and 0.5% Nonidet P-40 (NP-40) and supplemented with mammalian protease inhibitors. After centrifugation, supernatant was collected and pre-cleared with 50 µl protein-A-agarose for 1 h at 4ºC. Pre-cleared supernatants were incubated

with either α-myc antibody or preimmune rabbit sera overnight at 4ºC. The next day, 40 μl (50% slurry) of washed suspended protein-A-agarose beads were added to each sample and incubated for a further 2 h at 4ºC. Beads were pelleted, washed and resuspended in 40 μl of Laemmli sample buffer, and boiled for 5 min at 95ºC. Proteins in immunoprecipitated samples were resolved on a 12% gel, transferred to nitrocellulose membrane and probed with *Tat* or α-myc antibodies.

2.10 Statistics

All results are expressed as the means ± S.E. For analysis of $\Delta\Psi_m$, ROS levels, BAG3 abundance, mitochondrial Ca^{2+} uptake and OCR, one-way analysis of variance was used. For analysis of myocyte contraction amplitudes as a function of group (WT and Tg26 for freshly isolated myocytes; WT-GFP, WT-BAG3, Tg26-GFP and Tg26-BAG3 for cultured myocytes), experimental condition (H/R, normoxia), and treatment (± Iso), three-way ANOVA was used. A commercially available software package (JMP Pro 13.0; SAS Institute, Cary, NC) was used. In all analyses, $p<0.05$ was taken to be statistically significant.

3. Results

3.1 Mitochondrial membrane potential (ΔΨm) and mitochondrial Ca^{2+} uptake are lower in Tg26 cardiac myocytes post-H/R

Ultra-structural damage in Tg26 cardiac mitochondria (Lewis, Grupp et al. 2000) would be expected to result in mitochondrial dysfunction. Although $\Delta\Psi_m$ was similar between permeabilized WT and Tg26 myocytes under basal conditions (Figs. 1A & 1B), after challenge with Ca^{2+} pulse (10 ¼M), $\Delta\Psi_m$ in Tg26 myocytes did not recover, in contrast to WT myocytes (Figs. 1A & 1C). Post-H/R, basal $\Delta\Psi_m$ was lower in Tg26 myocytes compared to WT myocytes (Figs. 1A & 1B). In addition, $\Delta\Psi_m$ measured after a 10 ¼M Ca^{2+} pulse and just before carbonyl cyanide m-chlorophenylhydrazone (CCCP) addition was significantly lower in Tg26-H/R than WT-H/R myocytes (Figs. 1A & 1C).

Because $\Delta\Psi_m$ was lower in Tg26 myocytes after Ca^{2+} challenge and H/R, we next assessed mitochondrial Ca^{2+} uptake in permeabilized myocytes. When challenged with repeated pulses of Ca^{2+}, WT-normoxic but not Tg26-normoxic myocytes were able to repeatedly lower extra-mitochondrial Ca^{2+} (Fig. 1D). This observation suggests that the mitochondrial Ca^{2+} uniporter (MCU) activity was lower in Tg26 myocytes since the driving force for Ca^{2+} uptake $\Delta\Psi_m$, was similar between WT and Tg26 myocytes under basal, normoxic conditions (Figs. 1A & 1B). Compared to WT-normoxic myocytes, the rate of mitochondrial Ca^{2+} uptake (Fig. 1E) and the amount of mitochondrial Ca^{2+} accumulated (Fig. 1F) were very low in WT-H/R, Tg26-normoxic and Tg26-H/R myocytes.

We next measured $\Delta\Psi_m$ in intact cardiac myocytes loaded with TMRM by confocal microscopy. Similar to permeabilized myocytes (Figs. 1A & 1B), $\Delta\Psi_m$ was similar between non-permeabilized WT and Tg26 myocytes under basal normoxic conditions (Fig. 2). Post-H/R, $\Delta\Psi_m$ was significantly lower in Tg26 myocytes when compared to WT myocytes. Unlike digitonin-permeabilized WT myocytes (Fig. 1B), post-H/R intact WT myocytes did

not demonstrate a statistically significant decrease in $\Delta\Psi_m$ (Fig. 2). This apparent "discrepancy" is likely due to mitochondrial respiration was not substrate-limited in permeabilized myocytes (supplemented with 10 mM succinate) whereas endogenous substrates were utilized by intact myocytes.

3.2 Oxygen consumption rate and ATP levels are lower in Tg26 cardiac myocytes

Defective mitochondrial Ca^{2+} uptake in Tg26-normoxic myocytes would be expected to adversely affect OCR since constitutive, low level mitochondrial Ca^{2+} uptake is essential in maintaining cellular bioenergetics (Cardenas et al. 2010). Indeed, under normoxic conditions, both basal and maximal OCRs were significantly lower in Tg26-normoxic myocytes when compared to WT-normoxic myocytes (Fig. 3A to D). Levels of NADH dehydrogenase (ubiquinone) 1α subcomplex 4-like 2 (NDUFA4L2), a subunit of Complex I, were much reduced in Tg26 myocytes (Fig. 3E). ATP levels were significantly lower in Tg26 hearts when compared to WT hearts (Fig. 3F). Post-H/R, basal OCR was reduced in both WT and Tg26 myocytes (Fig. 3B). Interestingly post-H/R, maximal OCR although decreased in WT myocytes, was unchanged in Tg26 myocytes (Fig. 3C). This is likely due to the already low maximal OCR observed in Tg26-normoxic myocytes.

3.3 Mitochondrial superoxide levels are higher in Tg26 myocytes post-H/R: Rescue by BAG3

Mitochondria are the major source of ROS in cardiac myocytes. Since Tg26 myocytes exhibited mitochondrial dysfunction (reduced mitochondrial Ca^{2+} uptake; lower OCR and $\Delta\Psi_m$ post-H/R), we measured mitochondrial ROS in myocytes using MitoSOX Red, which detects mitochondrial superoxide anion ($O_2^{\cdot -}$)(Miller et al. 2014). Because we have previously demonstrated that BAG3 expression reverses contractile dysfunction in adult mouse myocytes overexpressing *Tat* (Cheung et al. 2015), and that BAG3 is intimately involved in mitochondrial quality control in cardiac myocytes (Tahrir et al. 2017), in this series of experiments we used WT and Tg26 myocytes infected with adenovirus and cultured for 24h to allow expression of exogenous BAG3 or GFP (control). After 24h of culture, BAG3 levels were ~50% higher in myocytes expressing exogenous BAG3 when compared to myocytes expressing GFP (Fig. 4A). Under normoxic conditions, there were no significant differences in $O_2^{\cdot -}$ levels among WT-GFP, WT-BAG3, Tg26-GFP and Tg26-BAG3 myocytes although $O_2^{\cdot -}$ levels tended to be higher in Tg26 myocytes (Fig. 4B). Post-H/R, $O_2^{\cdot -}$ levels were elevated in both WT-GFP and Tg26-GFP myocytes. In particular, post-H/R Tg26-GFP myocytes had significantly ($p<0.01$) higher $O_2^{\cdot -}$ levels than WT-GFP myocytes (Fig. 4B), consistent with worse mitochondrial dysfunction observed in Tg26 myocytes. BAG3 overexpression significantly reduced the elevated $O_2^{\cdot -}$ levels post-H/R in WT and Tg26 myocytes close to those measured in normoxic myocytes (Fig. 4B).

3.4 Myocyte contraction is impaired post-H/R: Amelioration by BAG3

Endogenous BAG3 levels were similar between WT (40.4 ± 2.1 arbitrary units, n=4) and Tg26 (43.0 ± 3.4 arbitrary units, n=4) hearts (Fig. 5A; p=0.54). In freshly isolated myocytes incubated under normoxic conditions, there were no differences in single myocyte contraction amplitudes between WT and Tg26 myocytes, both in the absence or presence of isoproterenol (Fig. 5B; p=0.25). This observation is consistent with our previous report that

in vivo cardiac contractility (+dP/dt and –dP/dt measured with escalating doses of isoproterenol) and in vitro myocyte contraction dynamics were similar between WT and Tg26 mice (Cheung et al. 2015). Post-H/R, myocyte contraction amplitudes were significantly lower (H/R effect, $p<0.0001$) in both WT and Tg26 myocytes when compared to their normoxic counterparts. Post-H/R and in the presence of isoproterenol, Tg26 myocytes contracted significantly less ($p<0.025$) than WT myocytes (Fig. 5B).

To ascertain if BAG3 overexpression can ameliorate contractile dysfunction brought on by H/R, we used WT and Tg26 myocytes infected with adenovirus expressing either GFP or BAG3 and cultured for 24h. Similar to freshly isolated myocytes, there were no differences in contraction amplitudes between normoxic WT-GFP and Tg26-GFP myocytes (Fig. 6; $p<0.37$). Across the 4 groups of myocytes (WT-GFP, WT-BAG3, Tg26-GFP and Tg26-BAG3), H/R significantly reduced maximal contraction amplitudes (Fig. 6; H/R effect, $p<0.0001$), while isoproterenol significantly increased maximal contraction amplitudes (Iso effect, $p<0.0001$). Most interesting is the observation that under double stress (H/R and isoproterenol), Tg26-GFP myocytes contracted significantly less that WT-GFP myocytes (Fig. 6; WT-GFP vs. Tg26-GFP, $p<0.001$).

Under normoxic conditions, BAG3 overexpression had no significant effect on maximal contraction amplitudes in both WT and Tg26 myocytes (Fig. 6; $p<0.20$), similar to what we previously reported on the effects of BAG3 overexpression in WT myocytes (Cheung et al. 2015). BAG3 overexpression significantly enhanced contraction amplitudes in WT myocytes post-H/R and in the presence of isoproterenol (Fig. 6; WT-GFP vs. WT-BAG3, $p<0.025$). BAG3 overexpression also increased contraction amplitudes in Tg26 myocytes post-H/R and in the presence of isoproterenol (Fig. 6; Tg26-GFP vs. Tg26-BAG3, $p<0.045$). Most significant is that post-H/R and in the presence of isoproterenol, BAG3 overexpression restored maximal contraction amplitudes in Tg26 myocytes to the values measured in WT myocytes (Fig. 6; WT-BAG3 vs. Tg26-BAG3, $p=0.45$).

3.5 Physical association between BAG3 and *Tat*

Our previous observation that BAG3 overexpression improved contractile dysfunction in WT adult mouse ventricular myocytes overexpressing *Tat* (Cheung et al. 2015), together with our current results that post-H/R and in the presence of isoproterenol, BAG3 overexpression restored contraction amplitudes in Tg26 myocytes (also expressing *Tat*) to normal, suggest that the beneficial effects of BAG3 may be mediated by direct interaction with *Tat*. Indeed, co-immunoprecipitation experiments demonstrated physical association between BAG3 and *Tat* (Fig. 7).

4. Discussion

The Tg26 mouse with its complement of HIV-1 proteins (Kopp et al. 1992, Niu et al. 2014) but absence of infectious virus, and normal to minimally perturbed cardiac function measured at baseline (Lewis et al. 2000, Cheung et al. 2015), mimics the contemporary HIV-1 infected patient on cART. Of the HIV-1 proteins, *Tat* has been most often implicated in the development of HIV cardiomyopathy. For example, high levels of cardiac-specific *Tat* overexpression in hemizygous mice resulted in 46% increase in LV mass and reduction in

fractional shortening (FS) from 40 to 28% at 90 days (Raidel et al. 2002). The pathogenetic role of *Tat* in reducing cardiac contractility was independently confirmed in adult mouse LV myocytes overexpressing *Tat* by adenoviral transduction, in which contraction amplitude, shortening and re-lengthening velocities were all reduced when compared to myocytes overexpressing GFP (Cheung et al. 2015). Another important observation is that at 210 days, unambiguous mitochondrial damage (cristae and matrix disruption, lamellar figures, incomplete fusion, and undivided mitochondria) was observed in mitochondria of *Tat*-overexpressed hearts (Raidel et al. 2002). This led us to postulate that interference with mitochondrial bioenergetics is a plausible mechanism by which *Tat* exerts its negative inotropic effects. Indeed, when compared to NRVMs overexpressing GFP, NRVMs overexpressing *Tat* had lower OCR, reduced mitochondrial Ca^{2+} uptake and increased ROS levels (Tahrir et al. 2018). Using a fundamentally different approach, Lecoeur et al. (2012) demonstrated that when isolated mouse heart mitochondria was exposed to synthetic full-length *Tat*, mitochondrial swelling developed, $\Delta\Psi_m$ was rapidly dissipated and OCR was significantly reduced.

The first major finding is that under basal conditions, when compared to WT myocytes, Tg26 myocytes had depressed mitochondrial Ca^{2+} uptake, markedly decreased levels of Complex I (NDUFA4L2), reduced basal and maximal OCR and lower ATP levels, similar to the findings in NRVMs overexpressing *Tat* (Tahrir et al. 2018). These observations suggest that mitochondrial dysfunction in Tg26 myocytes is at least partly attributable to the effects of *Tat* in the mitochondria. Despite clear evidence of mitochondrial dysfunction, contractility both in the intact heart (Lewis et al. 2000, Cheung et al. 2015) as well as in isolated cardiac myocytes (Cheung et al. 2015), was not different between WT and Tg26 mice under basal conditions, suggesting perturbation in mitochondrial bioenergetics in Tg26 hearts was not severe enough to manifest as detectable changes in contractility under resting conditions. By contrast, when *Tat* was expressed at high levels in the transgenic murine heart, severe ultra-structural damage was observed in the mitochondria at >210 days and was temporally associated with decreases in FS (Raidel et al. 2002). Collectively, these observations suggest that the level of *Tat* expression may determine the degree of disturbance in mitochondrial bioenergetics, which when severe, leads to contractile dysfunction.

Hypoxia-reoxygenation stress is known to cause mitochondrial dysfunction and increase ROS levels in cardiac myocytes (Miller et al. 2014). Indeed, post-H/R, both WT and Tg26 myocytes demonstrated the expected reduction in mitochondrial Ca^{2+} uptake, $\Delta\Psi_m$ and OCR, and increases in $O_2^{\cdot -}$ levels. However, $\Delta\Psi_m$ was significantly lower and $O_2^{\cdot -}$ level was significantly higher in Tg26 myocytes when compared to WT myocytes post-H/R. Because of the already low OCR in Tg26 myocytes under normoxic conditions, the decrease in maximal OCR post-H/R was not as large in Tg26 myocytes (~40%) when compared to WT myocytes (~60%). These observations suggest that the already compromised mitochondria in Tg26 myocytes suffered worse damage when subjected to stress. More severe mitochondrial dysfunction in Tg26 myocytes post-H/R was manifested as lower maximal contraction amplitude especially in the presence of isoproterenol. In this context, it is interesting to note that cardiac function in Tg26 mice did not return to normal post-stress (open heart surgery), in contrast to WT mice (Cheung et al. 2015).

Although levels of BAG3 are similar between WT and Tg26 hearts, downregulation of BAG3 results in significant decrease in +dP/dt in Tg26 but not WT hearts (Cheung et al. 2015). On the other hand, overexpression of BAG3 rescues contractile dysfunction in adult myocytes overexpressing *Tat* (Cheung et al. 2015). These observations suggest interaction between *Tat* and BAG3 in HIV-1 infected hearts. Indeed, our co-immunoprecipitation results demonstrated physical association between *Tat* and BAG3 in cardiomyocytes. One of the loci of interaction between *Tat* and BAG3 is likely the mitochondrion since: (i) *Tat* induces ultrastructural damage in mitochondria (Raidel et al. 2002) and disrupts mitochondrial bioenergetics and mitochondrial quality control (Tahrir et al. 2018); (ii) BAG3 is intimately involved in mitochondrial quality control and is critical for the maintenance of mitochondrial homeostasis under stress (Tahrir et al. 2017); and (iii) Tg26 hearts have more ultrastructurally damaged mitochondria (Lewis et al. 2000) and exhibit mitochondrial dysfunction under basal conditions. Thus the third major finding of the present study is that BAG3 overexpression decreased the elevated $O_2^{\cdot -}$ levels in Tg26 myocytes post-H/R to those observed in normoxic myocytes. Improved mitochondrial function in Tg26 myocytes post-H/R by BAG3, enhanced β1 adrenergic receptor coupling with L-type Ca^{2+} channel by BAG3 (Feldman et al. 2016), and increased autophagy flux in injured cardiomyocytes by BAG3 (Su et al. 2016), may all contribute to improved contractile function when compared to control Tg26-GFP myocytes (Fig. 8). Collectively, our observations suggest that in HIV-1 infected hearts, there is a fine balance of interaction between BAG3 and *Tat* so that although there is evidence of altered mitochondrial function and reduced ATP levels, myocyte contractility is maintained. Imposition of additional stresses such as hypoxia/reoxygenation, BAG3 downregulation, adrenergic overdrive, or surgery, disrupts this fine balance and results in worse mitochondrial bioenergetics, increased oxidative stress and overt contractile dysfunction. Our results also point to the rationale of BAG3 upregulation or enhanced BAG3 activity as a therapeutic modality for HIV-1 associated cardiomyopathy. In this context, it should be noted that BAG3 overexpression in normal WT myocytes did not affect contraction amplitude, shortening or re-lengthening velocities [current results and previous study (Cheung et al. 2015)], suggesting lack of adverse effects on cardiac contractility if BAG3 is used as a therapeutic modality.

In summary, under basal conditions, mitochondrial function in Tg26 myocytes was abnormal although myocyte contractility was similar to that observed in WT myocytes. After hypoxia/reoxygenation, Tg26 myocytes had the lowest mitochondrial membrane potential and highest superoxide levels, and with added adrenergic stress, the worst myocyte contractile dynamics. Overexpression of BAG3 which physically associated with *Tat* reduced superoxide levels and improved myocyte contractility in Tg26 myocytes after hypoxia-reoxygenation injury. We conclude that persistent HIV-1 infection negatively impacts on cardiac mitochondrial function and that BAG3 likely has a therapeutic role in ameliorating AIDS cardiomyopathy.

Acknowledgment

This work was supported in part by the National Institutes of Health Grants RO1-HL123093, RO1-HL137426, RO1-HL86699 and PO1-HL91799 (Project 2). Core facilities were provided by Comprehensive NeuroAIDS Center P30-MH92177 at Temple University.

8. References

Barbaro G, Di Lorenzo G, Soldini M, Giancaspro G, Grisorio B, Pellicelli A and Barbarini G 1999 Intensity of myocardial expression of inducible nitric oxide synthase influences the clinical course of human immunodeficiency virus-associated cardiomyopathy. Gruppo Italiano per lo Studio Cardiologico dei pazienti affetti da AIDS (GISCA). Circulation 100(9): 933–939. [PubMed: 10468523]

Barnabei MS, Palpant NJ and Metzger JM 2010 Influence of genetic background on ex vivo and in vivo cardiac function in several commonly used inbred mouse strains. Physiol Genomics 42A(2): 103–113. [PubMed: 20627938]

Behl C 2016 Breaking BAG: The co-chaperone BAG3 in health and disease. Trends Pharmacol Sci 37(8): 672–688. [PubMed: 27162137]

Brinkman K, ter Hofstede HJ, Burger DM, Smeitink JA and Koopmans PP 1998 Adverse effects of reverse transcriptase inhibitors: mitochondrial toxicity as common pathway. AIDS 12(14): 1735–1744. [PubMed: 9792373]

Cardenas C, Miller RA, Smith I, Bui T, Molgo J, Muller M, Vais H, Cheung KH, Yang J, Parker I, Thompson CB, Birnbaum MJ, Hallows KR and Foskett JK 2010 Essential regulation of cell bioenergetics by constitutive InsP3 receptor Ca^{2+} transfer to mitochondria. Cell 142(2): 270–283. [PubMed: 20655468]

Cheung JY, Gordon J, Wang J, Song J, Zhang XQ, Tilley DG, Gao E, Koch WJ, Rabinowitz J, Klotman PE, Khalili K and Feldman AM 2015 Cardiac dysfunction in HIV-1 transgenic mouse: role of stress and BAG3. Clin Transl Sci 8(4): 305–310. [PubMed: 26300236]

Cheung JY, Thompson IG and Bonventre JV 1982 Effects of extracellular calcium removal and anoxia on isolated rat myocytes. Am J Physiol Cell Physiology 243: C184–C190.

Comereski CR, Kelly WA, Davidson TJ, Warner WA, Hopper LD and Oleson FB 1993 Acute cardiotoxicity of nucleoside analogs FddA and FddI in rats. Fundam Appl Toxicol 20(3): 360–364. [PubMed: 8504910]

Currie PF and Boon NA 2003 Immunopathogenesis of HIV-related heart muscle disease: current perspectives. AIDS 17 Suppl 1: S21–28. [PubMed: 12870527]

Eugenin EA, Morgello S, Klotman ME, Mosoian A, Lento PA, Berman JW and Schecter AD 2008 Human immunodeficiency virus (HIV) infects human arterial smooth muscle cells in vivo and in vitro: implications for the pathogenesis of HIV-mediated vascular disease. Am J Pathol 172(4): 1100–1111. [PubMed: 18310503]

Feldman AM, Gordon J, Wang J, Song J, Zhang XQ, Myers VD, Tilley DG, Gao E, Hoffman NE, Tomar D, Madesh M, Rabinowitz J, Koch WJ, Su F, Khalili K and Cheung JY 2016 BAG3 regulates contractility and Ca^{2+} homeostasis in adult mouse ventricular myocytes. J Mol Cell Cardiol 92: 10–20. [PubMed: 26796036]

Fiala M, Popik W, Qiao JH, Lossinsky AS, Alce T, Tran K, Yang W, Roos KP and Arthos J 2004 HIV-1 induces cardiomyopathyby cardiomyocyte invasion and gp120, Tat, and cytokine apoptotic signaling. Cardiovasc Toxicol 4(2): 97–107. [PubMed: 15371627]

Freiberg MS, Chang CH, Skanderson M, Patterson OV, DuVall SL, Brandt CA, So-Armah KA, Vasan RS, Oursler KA, Gottdiener J, Gottlieb S, Leaf D, Rodriguez-Barradas M, Tracy RP, Gibert CL, Rimland D, Bedimo RJ, Brown ST, Goetz MB, Warner A, Crothers K, Tindle HA, Alcorn C, Bachmann JM, Justice AC and Butt AA 2017 Association between HIV infection and the risk of heart failure with reduced ejection fraction and preserved ejection fraction in the antiretroviral therapy era: results from the veterans aging cohort study. JAMA Cardiol 2(5): 536–546. [PubMed: 28384660]

Grody WW, Cheng L and Lewis W, 1990 Infection of the heart by the human immunodeficiency virus. Am J Cardiol 66(2): 203–206. [PubMed: 2371952]

Hoffman NE, Miller BA, Wang J, Elrod JW, Rajan S, Gao E, Song J, Zhang XQ, Hirschler-Laszkiewicz I, Shanmughapriya S, Koch WJ, Feldman AM, Madesh M and Cheung JY 2015 Ca^{2+} entry via Trpm2 is essential for cardiac myocyte bioenergetics maintenance. Am J Physiol Heart Circ Physiol 308(6): H637–650. [PubMed: 25576627]

Irrinki KM, Mallilankaraman K, Thapa RJ, Chandramoorthy HC, Smith FJ, Jog NR, Gandhirajan RK, Kelsen SG, Houser SR, May MJ, Balachandran S and Madesh M 2011 Requirement of FADD, NEMO, and BAX/BAK for aberrant mitochondrial function in tumor necrosis factor alpha-induced necrosis. Mol Cell Biol 31(18): 3745–3758. [PubMed: 21746883]

Klotman PE and Notkins AL 1996 Transgenic models of human immunodeficiency virus type-1. Curr Top Microbiol Immunol 206: 197–222. [PubMed: 8608718]

Knezevic T, Myers VD, Gordon J, Tilley DG, Sharp TE, 3rd, Wang J, Khalili K, Cheung JY and Feldman AM 2015 BAG3: a new player in the heart failure paradigm. Heart Fail Rev 20: 423–434. [PubMed: 25925243]

Knezevic T, Myers VD, Su F, Wang J, Song J, Zhang XQ, Gao E, Gao G, Muniswamy M, Gupta MK, Gordon J, Weiner KN, Rabinowitz J, Ramsey FV, Tilley DG, Khalili K, Cheung JY and Feldman AM 2016 Adeno-associated virus serotype 9-driven expression of BAG3 improves left ventricular function in murine hearts with left ventricular dysfunction secondary to a myocardial infarction. JACC Basic Transl Sci 1(7): 647–656. [PubMed: 28164169]

Kopp JB, Klotman ME, Adler SH, Bruggeman LA, Dickie P, Marinos NJ, Eckhaus M, Bryant JL, Notkins AL and Klotman PE 1992 Progressive glomerulosclerosis and enhanced renal accumulation of basement membrane components in mice transgenic for human immunodeficiency virus type 1 genes. Proc Natl Acad Sci U S A 89(5): 1577–1581. [PubMed: 1542649]

Lecoeur H, Borgne-Sanchez A, Chaloin O, El-Khoury R, Brabant M, Langonne A, Porceddu M, Briere JJ, Buron N, Rebouillat D, Pechoux C, Deniaud A, Brenner C, Briand JP, Muller S, Rustin P and Jacotot E 2012 HIV-1 Tat protein directly induces mitochondrial membrane permeabilization and inactivates cytochrome c oxidase. Cell Death Dis 3: e282. [PubMed: 22419111]

Lewis W 2003 Use of the transgenic mouse in models of AIDS cardiomyopathy. AIDS 17 Suppl 1: S36–45. [PubMed: 12870529]

Lewis W, Grupp IL, Grupp G, Hoit B, Morris R, Samarel AM, Bruggeman L and Klotman P 2000 Cardiac dysfunction occurs in the HIV-1 transgenic mouse treated with zidovudine. Lab Invest 80(2): 187–197. [PubMed: 10701688]

Lipshultz SE, Fox CH, Perez-Atayde AR, Sanders SP, Colan SD, McIntosh K and Winter HS 1990 "Identification of human immunodeficiency virus-1 RNA and DNA in the heart of a child with cardiovascular abnormalities and congenital acquired immune deficiency syndrome. Am J Cardiol 66(2): 246–250. [PubMed: 2371963]

Mallilankaraman K, Doonan P, Cardenas C, Chandramoorthy HC, Muller M, Miller R, Hoffman NE, Gandhirajan RK, Molgo J, Birnbaum MJ, Rothberg BS, Mak DO, Foskett JK and Madesh M 2012 MICU1 is an essential gatekeeper for MCU-mediated mitochondrial Ca^{2+} uptake that regulates cell survival. Cell 151(3): 630–644. [PubMed: 23101630]

Manga P, McCutcheon K, Tsabedze N, Vachiat A and Zachariah D 2017 HIV and nonischemic heart disease. J Am Coll Cardiol 69(1): 83–91. [PubMed: 28057254]

McKenzie R, Fried MW, Sallie R, Conjeevaram H, Di Bisceglie AM, Park Y, Savarese B, Kleiner D, Tsokos M, Luciano C and et al. 1995 Hepatic failure and lactic acidosis due to fialuridine (FIAU), an investigational nucleoside analogue for chronic hepatitis B. N Engl J Med 333(17): 1099–1105. [PubMed: 7565947]

Miller BA, Hoffman NE, Merali S, Zhang XQ, Wang J, Rajan S, Shanmughapriya S, Gao E, Barrero CA, Mallilankaraman K, Song J, Gu T, Hirschler-Laszkiewicz I, Koch WJ, Feldman AM, Madesh M and Cheung JY 2014 TRPM2 channels protect against cardiac ischemia-reperfusion injury: role of mitochondria. J Biol Chem 289(11): 7615–7629. [PubMed: 24492610]

Miller BA, Wang J, Hirschler-Laszkiewicz I, Gao E, Song J, Zhang XQ, Koch WJ, Madesh M, Mallilankaraman K, Gu T, Chen SJ, Keefer K, Conrad K, Feldman AM and Cheung JY 2013 The second member of transient receptor potential-melastatin channel family protects hearts from ischemia-reperfusion injury. Am J Physiol Heart Circ Physiol 304(7): H1010–1022. [PubMed: 23376831]

Mocroft A, Ledergerber B, Katlama C, Kirk O, Reiss P, d'Arminio Monforte A, Knysz B, Dietrich M, Phillips AN, Lundgren JD and Euro SSG 2003 Decline in the AIDS and death rates in the EuroSIDA study: an observational study. Lancet 362(9377): 22–29. [PubMed: 12853195]

Mukhopadhyay P, Rajesh M, Hasko G, Hawkins BJ, Madesh M and Pacher P 2007 Simultaneous detection of apoptosis and mitochondrial superoxide production in live cells by flow cytometry and confocal microscopy. Nat Protoc 2(9): 2295–2301. [PubMed: 17853886]

Niu F, Yao H, Zhang W, Sutliff RL and Buch S 2014 Tat 101-mediated enhancement of brain pericyte migration involves platelet-derived growth factor subunit B homodimer: implications for human immunodeficiency virus-associated neurocognitive disorders. J Neurosci 34(35): 11812–11825. [PubMed: 25164676]

Pozzan G, Pagliari C, Tuon FF, Takakura CF, Kauffman MR and Duarte MI 2009 Diffuse-regressive alterations and apoptosis of myocytes: possible causes of myocardial dysfunction in HIV-related cardiomyopathy. Int J Cardiol 132(1): 90–95. [PubMed: 18222550]

Raidel SM, Haase C, Jansen NR, Russ RB, Sutliff RL, Velsor LW, Day BJ, Hoit BD, Samarel AM and Lewis W 2002 Targeted myocardial transgenic expression of HIV Tat causes cardiomyopathy and mitochondrial damage. Am J Physiol Heart Circ Physiol 282(5): H1672–1678. [PubMed: 11959630]

Remick J, Georgiopoulou V, Marti C, Ofotokun I, Kalogeropoulos A, Lewis W and Butler J 2014 Heart failure in patients with human immunodeficiency virus infection: epidemiology, pathophysiology, treatment, and future research. Circulation 129(17): 1781–1789. [PubMed: 24778120]

Rosati A, Graziano V, De Laurenzi V, Pascale M and Turco MC 2011 BAG3: a multifaceted protein that regulates major cell pathways. Cell Death Dis 2: e141. [PubMed: 21472004]

Shah AP, Siedlecka U, Gandhi A, Navaratnarajah M, Al-Saud SA, Yacoub MH and Terracciano CM 2010 Genetic background affects function and intracellular calcium regulation of mouse hearts. Cardiovasc Res 87(4): 683–693. [PubMed: 20413651]

Song J, Zhang XQ, Wang J, Cheskis E, Chan TO, Feldman AM, Tucker AL and Cheung JY 2008 Regulation of cardiac myocyte contractility by phospholemman:Na^+/Ca^{2+} exchange vs. Na^+-K^+-ATPase. Am J Physiol Heart Circ Physiol 295: H1615–H1625. [PubMed: 18708446]

Su F, Myers VD, Knezevic T, Wang J, Gao E, Madesh M, Tahrir FG, Gupta MK, Gordon J, Rabinowitz J, Ramsey FV, Tilley DG, Khalili K, Cheung JY and Feldman AM 2016 Bcl-2-associated athanogene 3 protects the heart from ischemia/reperfusion injury. JCI Insight 1(19): e90931. [PubMed: 27882354]

Tahrir FG, Knezevic T, Gupta MK, Gordon J, Cheung JY, Feldman AM and Khalili K 2017 Evidence for the role of BAG3 in mitochondrial quality control in cardiomyocytes. J Cell Physiol 232(4): 797–805. [PubMed: 27381181]

Tahrir FG, Shanmughapriya S, Ahooyi TM, Knezevic T, Gupta MK, Kontos CD, McClung JM, Madesh M, Gordon J, Feldman AM, Cheung JY and Khalili K 2018 Dysregulation of mitochondrial bioenergetics and quality control by HIV-1 Tat in cardiomyocytes. J Cell Physiol 233(2): 748–758. [PubMed: 28493473]

Tucker AL, Song J, Zhang XQ, Wang J, Ahlers BA, Carl LL, Mounsey JP, Moorman JR, Rothblum LI and Cheung JY 2006 Altered contractility and $[Ca^{2+}]_i$ homeostasis in phospholemman-deficient murine myocytes: Role of Na^+/Ca^{2+} exchange. Am J Physiol Heart Circ Physiol 291: H2199–H2209. [PubMed: 16751288]

Ulbricht A and Hohfeld J 2013 Tension-induced autophagy: may the chaperone be with you. Autophagy 9(6): 920–922. [PubMed: 23518596]

van den Borne SW, van de Schans VA, Strzelecka AE, Vervoort-Peters HT, Lijnen PM, Cleutjens JP, Smits JF, Daemen MJ, Janssen BJ and Blankesteijn WM 2009 Mouse strain determines the outcome of wound healing after myocardial infarction. Cardiovasc Res 84(2): 273–282. [PubMed: 19542177]

Zhou YY, Wang SQ, Zhu WZ, Chruscinski A, Kobilka BK, Ziman B, Wang S, Lakatta EG, Cheng H and Xiao RP 2000 Culture and adenoviral infection of adult mouse cardiac myocytes: methods for cellular genetic physiology. Am J Physiol Heart Circ Physiol 279(1): H429–436. [PubMed: 10899083]

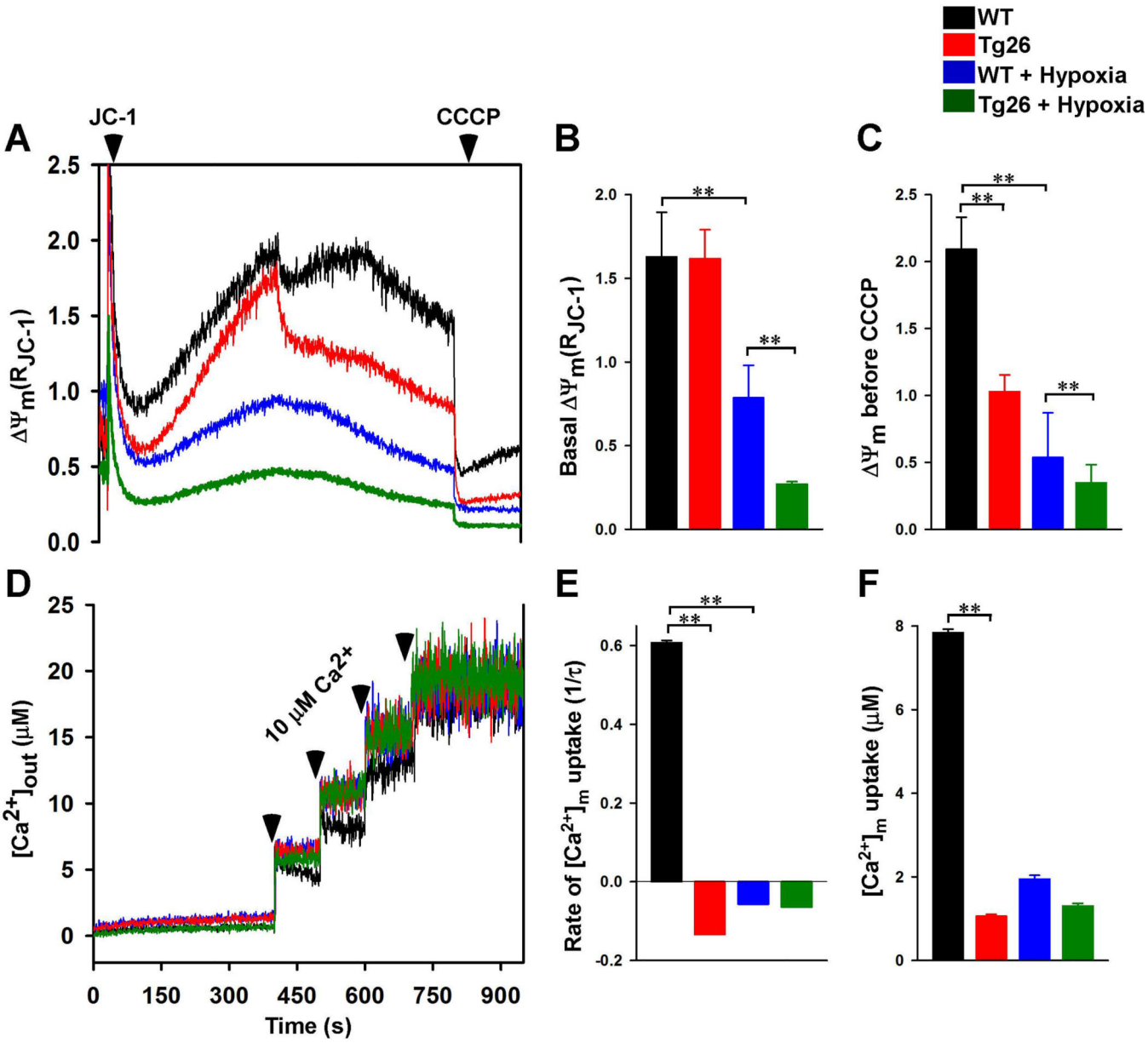

Figure 1.

Mitochondrial membrane potential and mitochondrial Ca2+ uptake are lower in permeabilized Tg26 myocytes after hypoxia/reoxygenation. LV myocytes isolated from WT and Tg26 mice were subjected to normoxia or hypoxia for 2 h followed by 30 min. of reoxygenation (Materials and Methods). Myocytes were permeabilized with digitonin and supplemented with succinate. A: the ratiometric indicator JC-1 was added at 20s and used to monitor ΔΨm. B & C: summary of basal ΔΨm and ΔΨm after 10 μM Ca2+ addition but before CCCP addition, respectively (n = 6 experiments from 3 mice in each group). D: the ratiometric dye Fura-FF was added at 0s and used to monitor extra-mitochondrial Ca2+. Repeated pulses of Ca2+ (10 μM) were added as indicated (arrows). The rate of mitochondrial Ca2+ uptake after the first Ca2+ pulse was measured. E & F: summary of

mitochondrial Ca2+ uptake rate and amount of Ca2+ uptake by mitochondria, respectively (n=6 experiments from 3 mice in each group). **p<0.01.

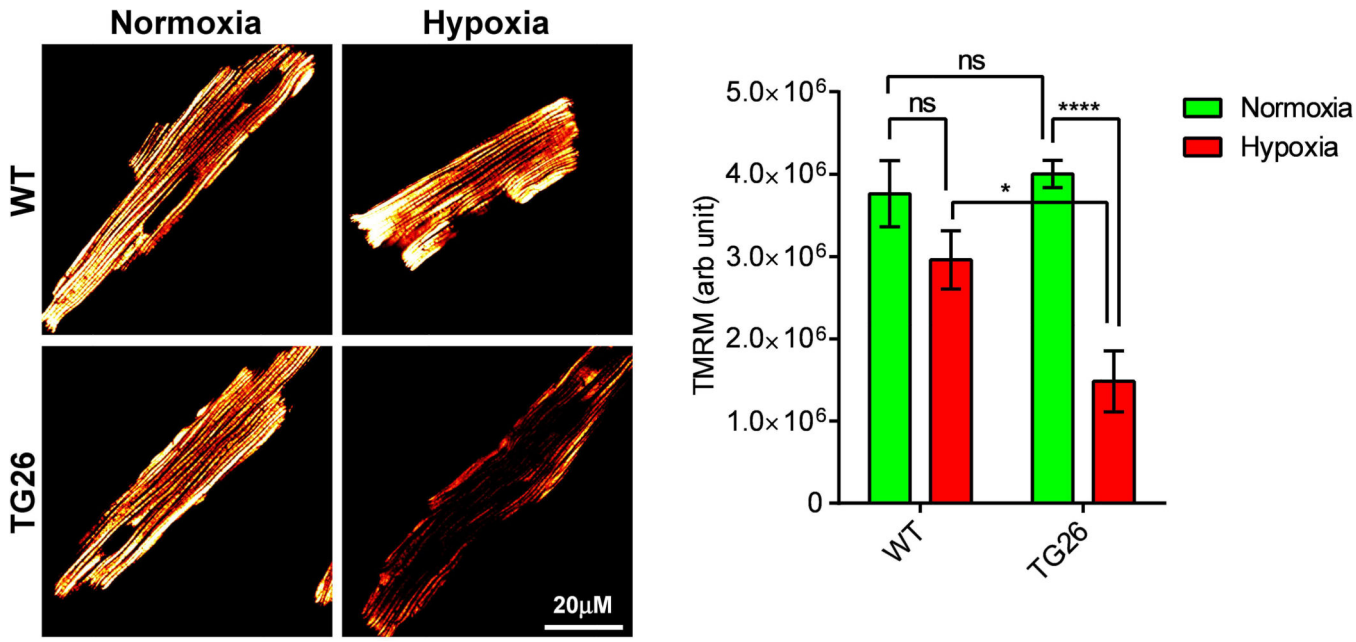

Figure 2.

Mitochondrial membrane potential is lower in intact Tg26 myocytes after hypoxia/reoxygenation. LV myocytes isolated from WT and Tg26 mice were subjected to normoxia or hypoxia for 2h followed by 30 min of reoxygenation. Myocytes were loaded with the mitochondrial membrane potential indicator TMRM (Materials and Methods). Confocal images (n=8 to 11 myocytes for each condition) were obtained and fluorescence signal intensities of TMRM were quantified in fluorescence arbitrary units. *p<0.05; ****p<0.001.

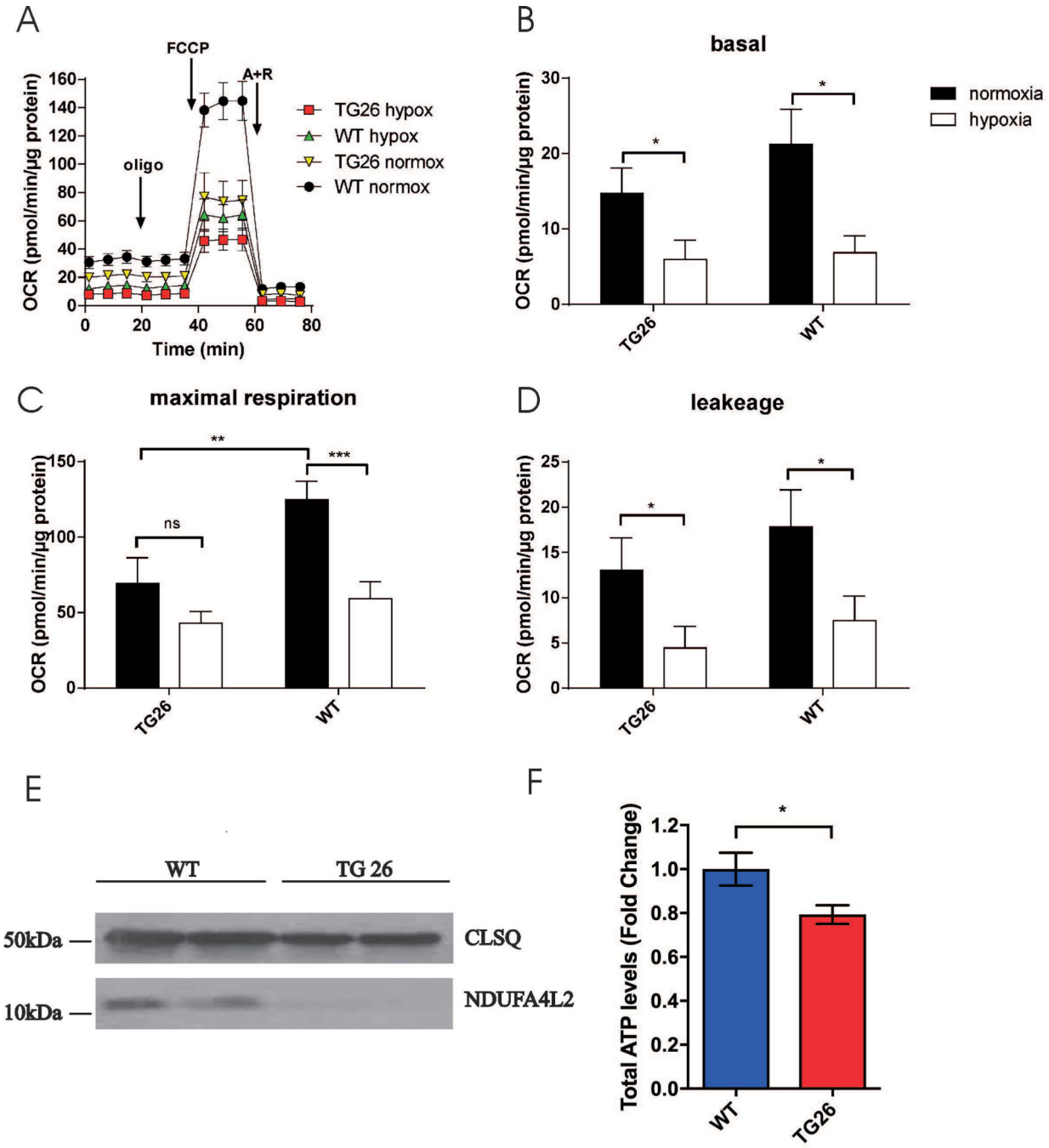

Figure 3.

Oxygen consumption rate and ATP levels are reduced in Tg26 hearts. O2 consumption rate (OCR) was measured in freshly isolated intact LV myocytes from WT and Tg26 mice (Materials and Methods). A: after basal OCR was obtained, oligomycin (1 µM) was added to inhibit F0F1ATPase (Complex V)(Point A). The uncoupler FCCP (1 µM) was then added (Point B), and maximal OCR was measured. Finally, antimycin A + rotenone (1 µM each) were added (Point C) to inhibit cytochrome bc1 complexes (Complex III) and NADH dehydrogenase (Complex I), respectively. Each point in the traces represents the average of

eight different wells. B, C & D: summary of basal OCR (B), ATP coupled respiration (C) and maximal OCR (D)(n = 3 WT and 3 Tg26 mice). E: Hearts from WT (blue) and Tg26 (red) mice were homogenized, and ATP levels were measured by CellTiter-Glo assay (n=3 each). *p<0.05, **p<0.01; ***p<0.001.

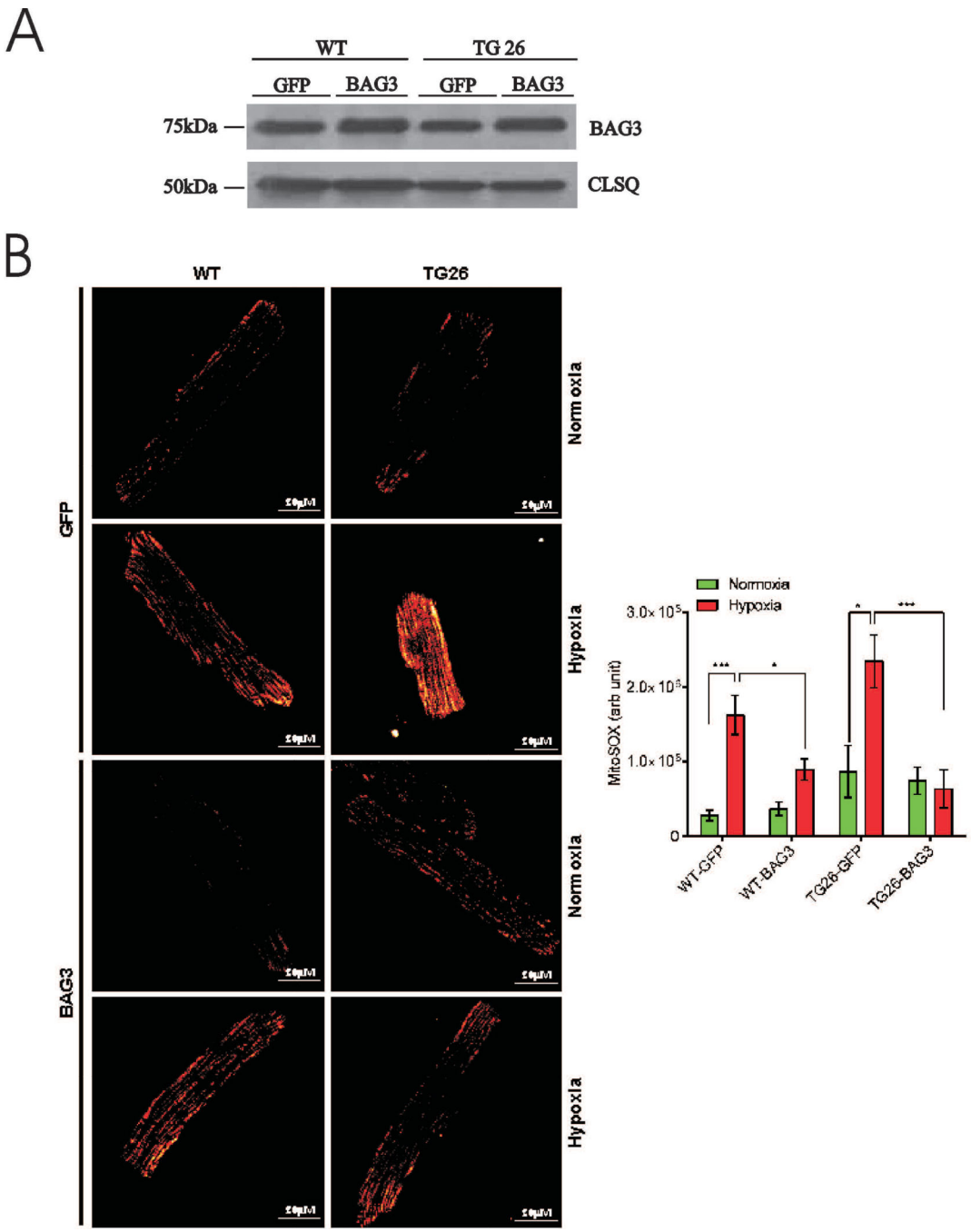

Figure 4.

Hypoxia/reoxygenation reduces oxygen consumption rate in WT and Tg26 myocytes. LV myocytes isolated from WT and Tg26 mice were subjected to normoxia or hypoxia for 2h followed by 30 min. of reoxygenation before OCR measurements as described in Fig. 3. Summaries of basal and maximal OCR for the 4 groups of myocytes (4 WT and 5 Tg26 mice) are shown. Also shown is the summary of proton leak (defined as OCR after oligomycin minus OCR after antimycin A and rotenone addition). *p<0.05; **p<0.01; ***p<0.001.

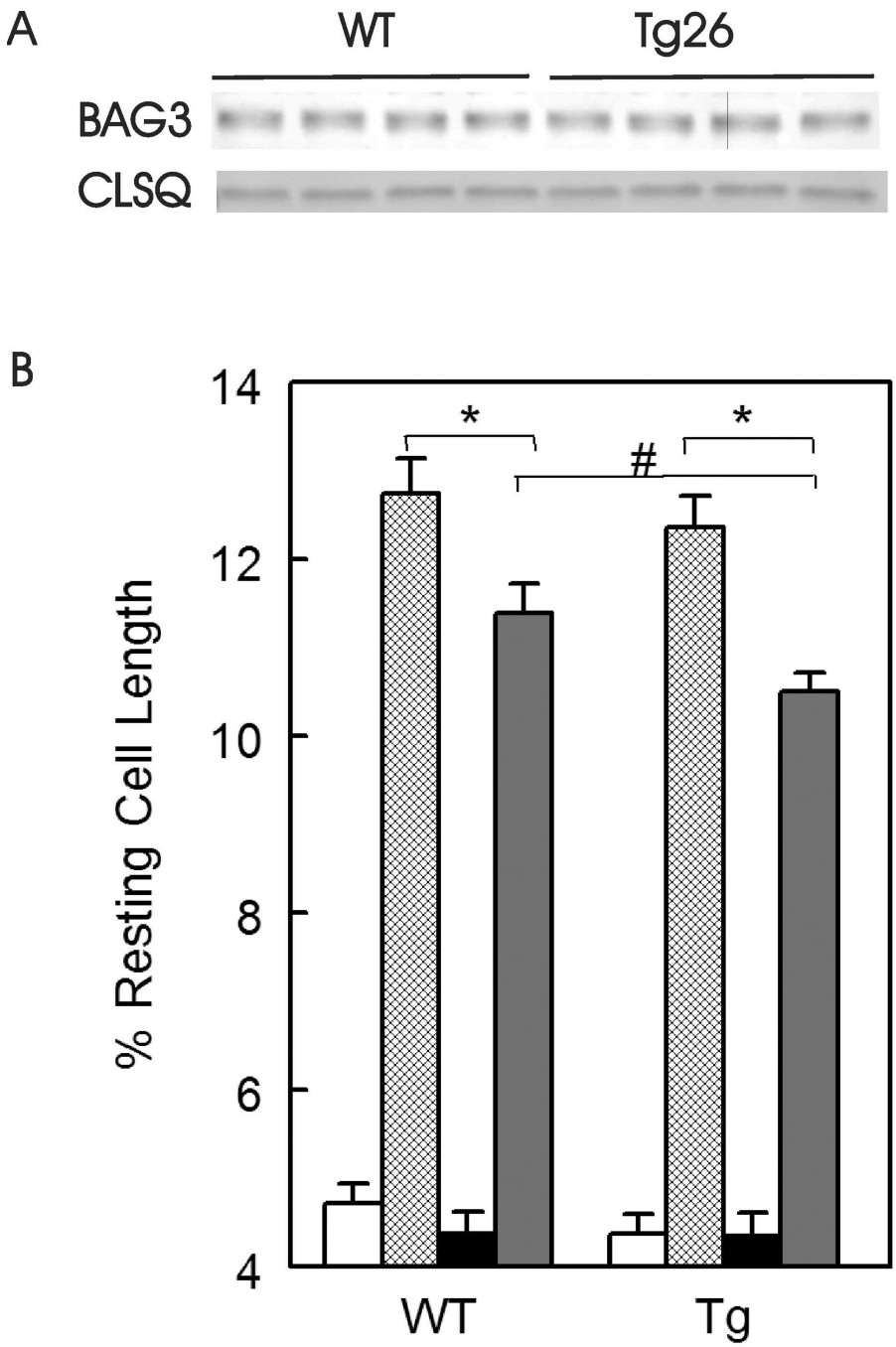

Figure 5.

Endogenous BAG3 levels are similar but myocyte contractility is lower in Tg26 myocytes after hypoxia/reoxygenation and isoproterenol. A: LV homogenates were prepared from WT and Tg26 hearts and BAG3 measured. Calsequestrin (CLSQ) was used as a loading control. B: Freshly isolated myocytes were paced to contract at 2 Hz, 370C and 1.8 mM [Ca2+]o (Materials and Methods), under normoxic conditions in the absence (open bars) and presence (hatched bars) of 1 μM isoproterenol (Iso), or subjected to 2 h of hypoxia followed by 30 min. of reoxygenation before contraction measurements in the absence (solid black

bars) and presence (solid gray bars) of 1 μM isoproterenol. Myocytes were isolated from 3 WT and 3 Tg26 mice. There are 23, 23, 24 and 25 WT-normoxic, WT-normoxic + Iso, WT-H/R and WT-H/R + Iso myocytes, respectively. Similarly, there are 21, 24, 22, and 27 Tg26-normoxic, Tg26-normoxic + Iso, Tg26-H/R and Tg26-H/R + Iso myocytes, respectively. Maximal contraction amplitude is given as % resting cell length. Means ± SE are shown. *$p<0.0001$, #$p<0.025$.

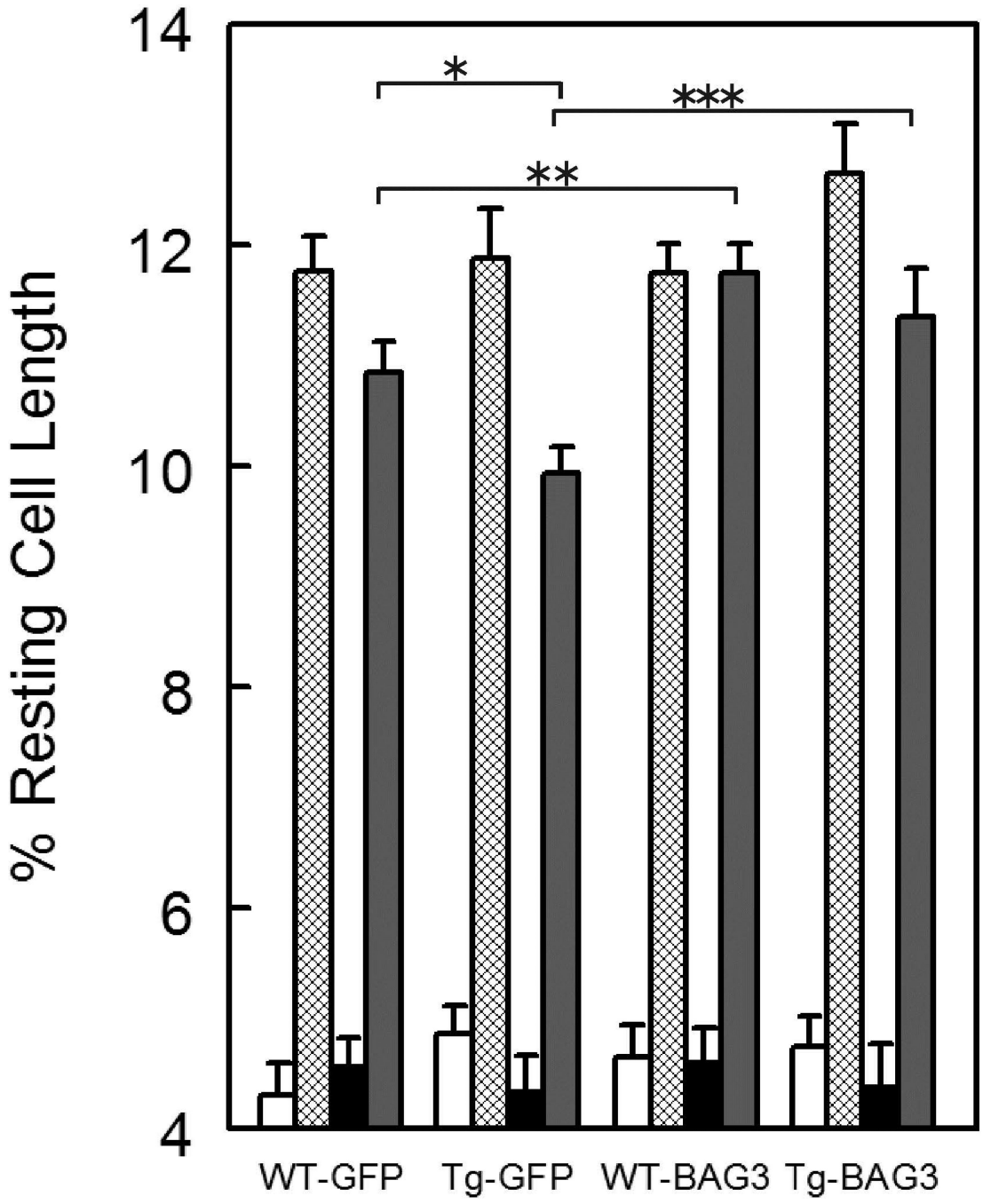

Figure 6.

BAG3 overexpression rescues contractile abnormality in Tg26 myocytes subjected to hypoxiareoxygenation and isoproterenol. Left ventricular myocytes isolated from WT (n=4 mice) and Tg26 (n=4 mice) hearts were infected with Adv-GFP or Adv-BAG3 and cultured for 24h (Materials and Methods) before contractility measurements (Figure 5). For cultured myocytes, duration of hypoxia was 30 min. followed by 30 min. of reoxygenation (Miller et al. 2014). Open bars: normoxia; hatched bars: normoxia + Iso; solid black bars: H/R; solid gray bars: H/R + Iso. For WT-GFP, there are 18, 22, 17 and 19 normoxic, normoxic + Iso,

H/R and H/R + Iso myocytes, respectively. For WT-BAG3, there are 18, 19, 16 and 20 normoxic, normoxic + Iso, H/R and H/R + Iso myocytes, respectively. For Tg26-GFP, there are 19, 24, 21 and 19 normoxic, normoxic + Iso, H/R and H/R + Iso myocytes, respectively. For Tg26-BAG3, there are 24, 22, 23 and 23 normoxic, normoxic + Iso, H/R and H/R + Iso myocytes, respectively. Maximal contraction amplitude is given as % resting cell length. Means ± SE are shown. *$p<0.001$, **$p<0.025$, ***$p<0.045$.

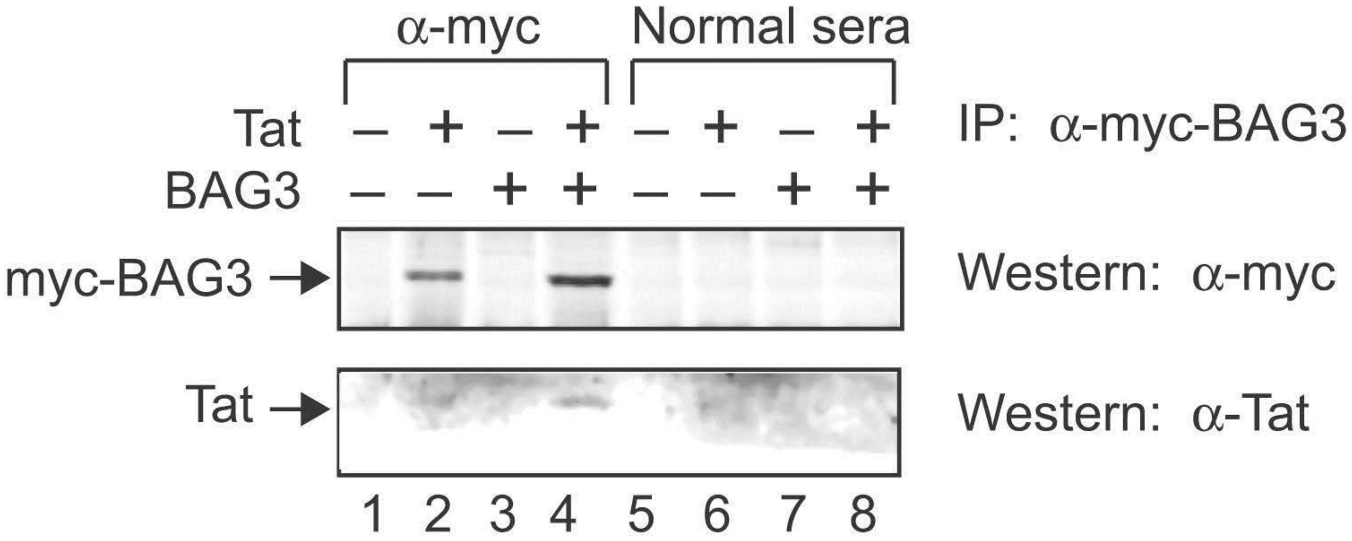

Figure 7.

Demonstration of association of Tat with BAG3 in transfected H9C2 cardiomyocytes by coimmunoprecipitation. H9C2 cardiomyocytes were transfected with pcDNA6 myc-BAG3 or pcDNA3 Tat, or both plasmids for 48 hours after which co-immunoprecipitation was performed (Materials and Methods). The control preimmune rabbit sera (Normal sera) failed to immunoprecipitate myc-tagged BAG3 or Tat (lanes 5 to 8). Using α-myc antibody, BAG3 was successfully immunoprecipitated (lanes 2 and 4) and Tat coimmunoprecipitated with BAG3 (lane 4).

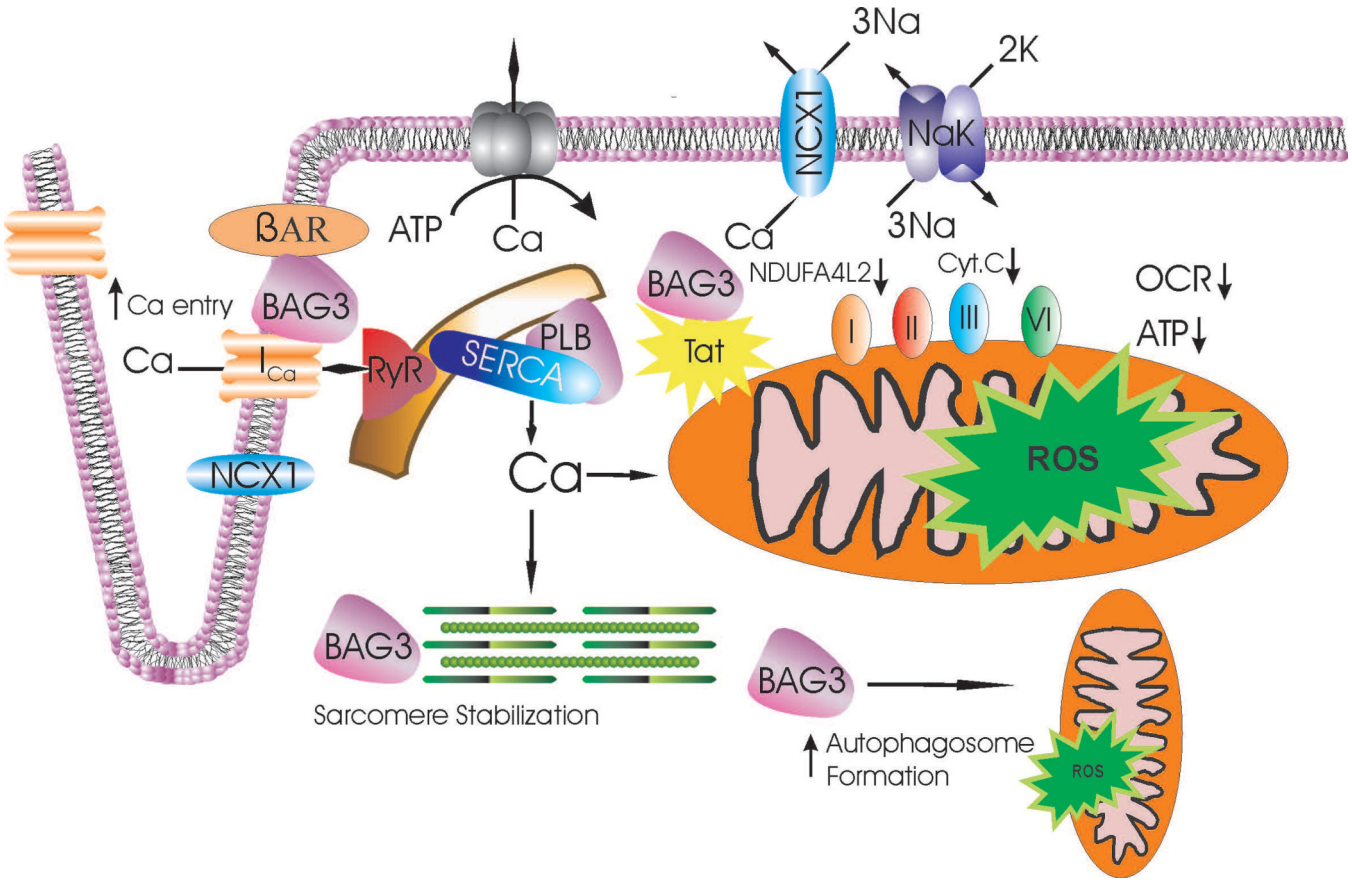

Figure 8.

Excitation-contraction coupling, mitochondrial function and mitophagy: targets for Tat and improvement by BAG3 in Tg26 myocytes. With depolarization, extracellular Ca2+ enters via L-type Ca2+ channel (ICa) and Na+/Ca2+ exchanger (NCX1)(both depicted as mainly situated in the t-tubules), causing Ca2+ release from the ryanodine receptor (RyR) in the sarcoplasmic reticulum (SR). Ca2+ binds to troponin to initiate myofilament contraction and ATP is consumed. During diastole, Ca2+ is pumped back to the SR by SR Ca2+-ATPase (SERCA) whose activity is modulated by phospholamban (PLB). The amount of Ca2+ that has entered during systole is extruded by Na+/Ca2+ exchanger and to a very minor extent, by sarcolemmal Ca2+-ATPase. The HIV-1 protein Tat impairs mitochondrial electron transport by reducing levels of Complex I (NDUFA4L2) and Complex III (cytochrome c) in the heart (Tahrir et al. 2018), resulting in decreased oxygen consumption rate (OCR) and ATP (Fig. 3), and increased ROS levels (Fig. 4). BAG3, by sequestering Tat as well as promoting autophagy (Su et al. 2016) and mitochondrial quality control (Tahrir et al. 2018), improves mitochondrial bioenergetics and reduces ROS (Fig. 4). In addition, BAG3 enhances β- adrenergic responsiveness and regulates activities of ion channels including the L-type Ca2+ channel (Feldman et al. 2016), allowing more Ca2+ to enter during systole. Finally, BAG3 enhances sarcomere stability (Ulbricht and Hohfeld 2013). These beneficial effects of BAG3 may all contribute to improve contractility of HIV-1 infected cardiac

myocytes under conditions of stress such as hypoxia-reoxygenation (increased ROS; Fig. 4) and adrenergic stimulation (Fig. 6).